

## Supplementary Material

### **Laminated ferroelectric polymer composites exhibiting synchronous ultrahigh discharge efficiency and energy density via utilizing multiple-interface barriers**

Jie Chen<sup>a</sup>, Xiaoyong Zhang<sup>a</sup>, Zhen Wang<sup>a</sup>, Weixing Chen<sup>a</sup>, Qibin Yuan<sup>b,\*</sup>, and Yifei Wang<sup>c,\*</sup>

<sup>a</sup> Shaanxi Key Laboratory of Optoelectronic Functional Materials and Devices, School of Materials Science and Chemical Engineering, Xi'an Technological University, Xi'an 710032, China

<sup>b</sup> School of Electronic Information and Artificial Intelligence, Shaanxi University of Science and Technology, Xi'an 710021, China

<sup>c</sup> Electrical Insulation Research Center, Institute of Materials Science, University of Connecticut, Storrs, Connecticut 06269, USA

\* Corresponding authors. [yuanqibin-sust@163.com](mailto:yuanqibin-sust@163.com) (Q. Yuan), [y.wang@uconn.edu](mailto:y.wang@uconn.edu) (Y. Wang)

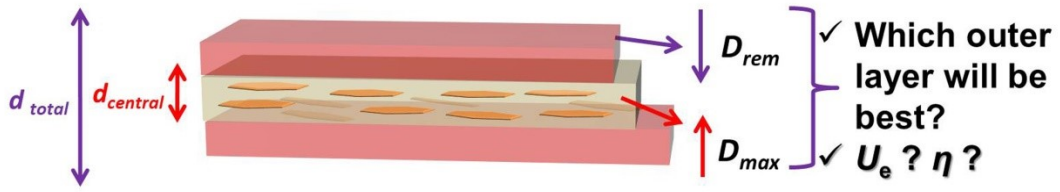


**Fig. S1.** Schematic illustration of tri-layered structure composite film.



**Fig. S2.** Optical images of a) P(VDF-HFP)-S, b) 50 wt% PMMA-S and c) PMMA-S, respectively.

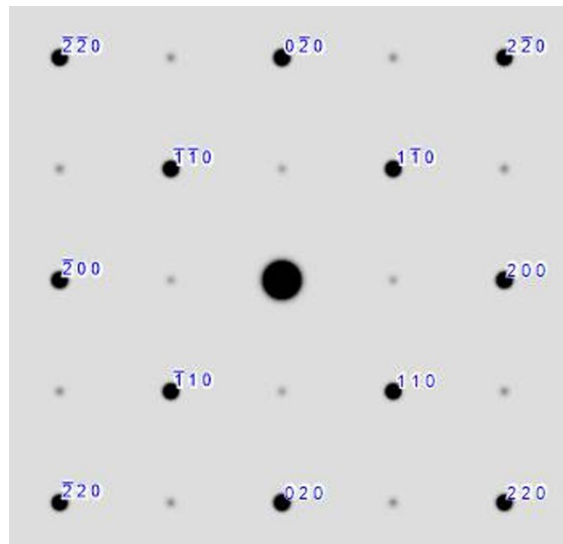


**Fig. S3.** SAED pattern of the prepared SrTiO<sub>3</sub>@PDA plates.

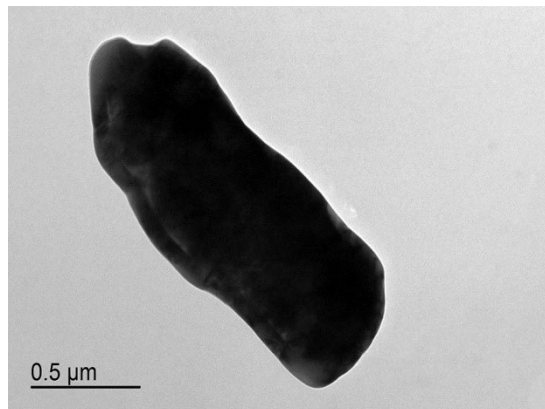


**Fig. S4.** TEM image of the prepared SrTiO<sub>3</sub>@PDA plates.

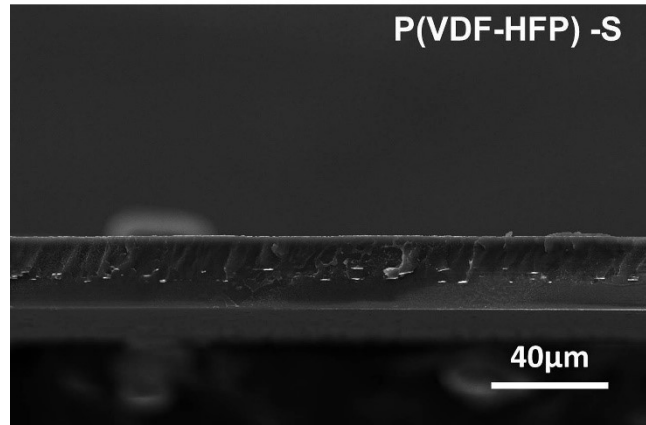


**Fig. S5.** Cross-section SEM image with a large scale of P(VDF-HFP)-S film, scale bar 40 μm.

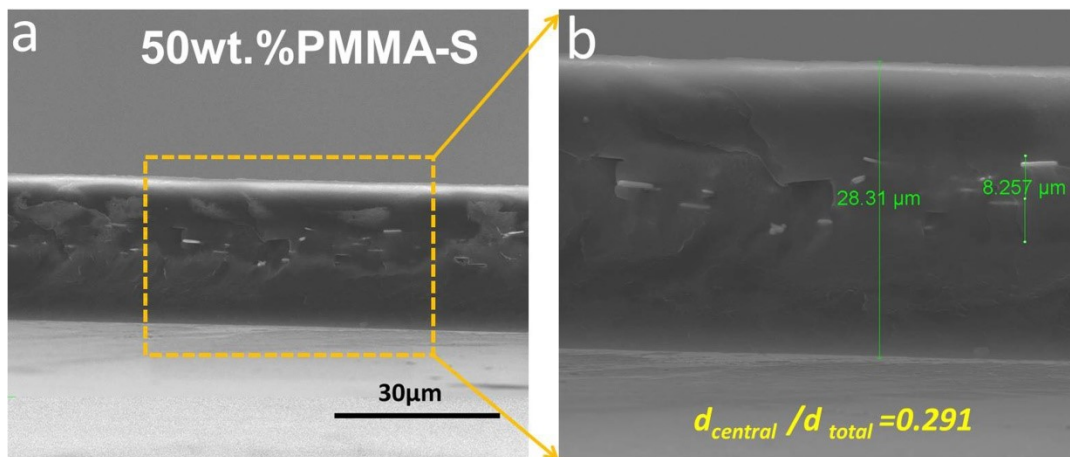


**Fig. S6.** a) Cross-section SEM image, (b) magnified SEM image of 50 wt.% PMMA-S film.

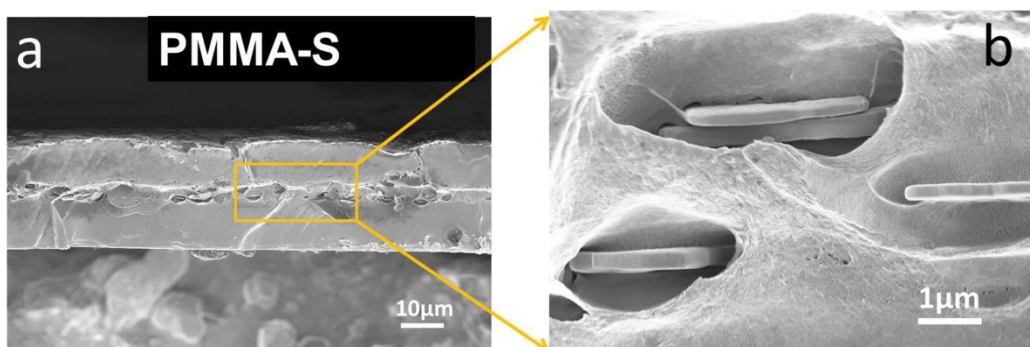


**Fig. S7.** a) Cross-section SEM image, (b) magnified SEM image of PMMA-S film.

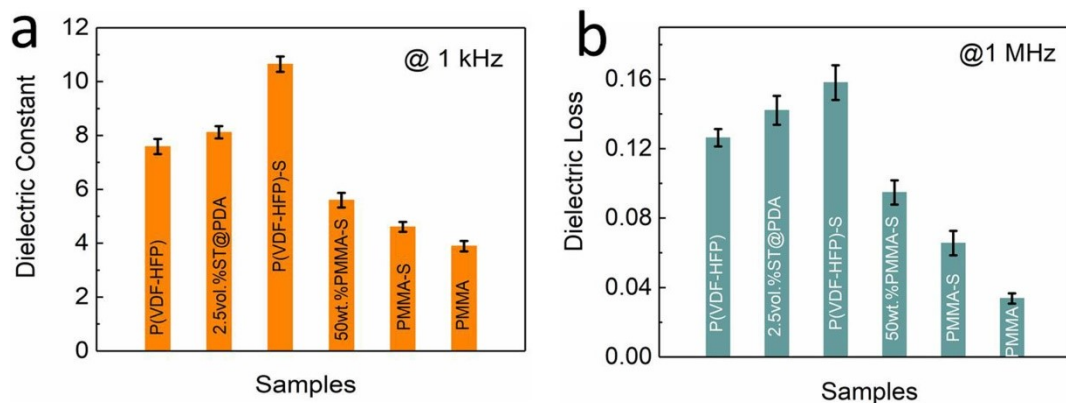


**Fig. S8.** a) dielectric constant at 1 kHz, b) dielectric loss at 1 MHz of the tri-layered configuration composites, single-layered configuration composite and pristine constituent polymers.

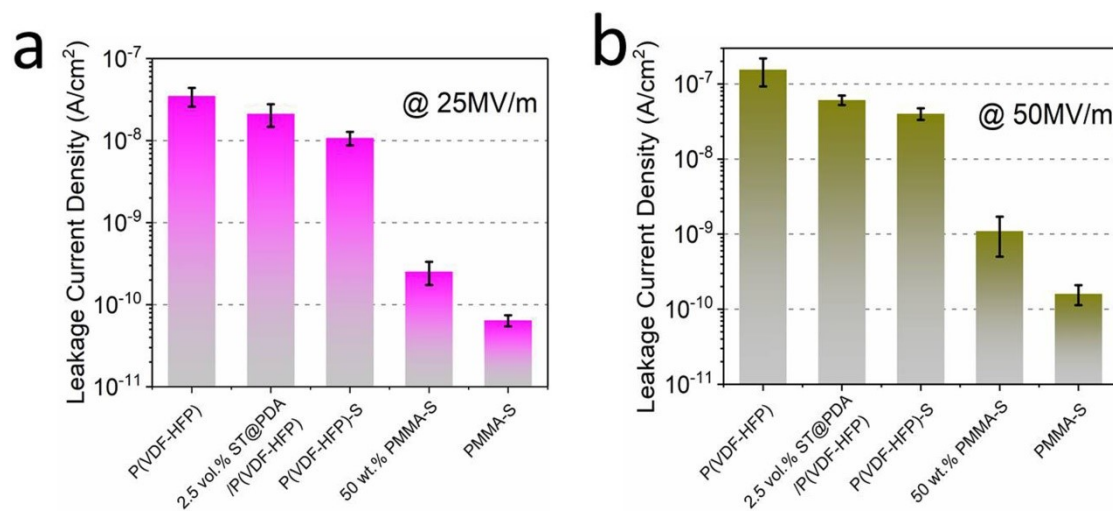


**Fig. S9.** Leakage current density a) measured at 25 MV m<sup>-1</sup> and b) measured at 50 MV m<sup>-1</sup> of tri-layered configuration composites, single-layered configuration composite, and pristine P(VDF-HFP).

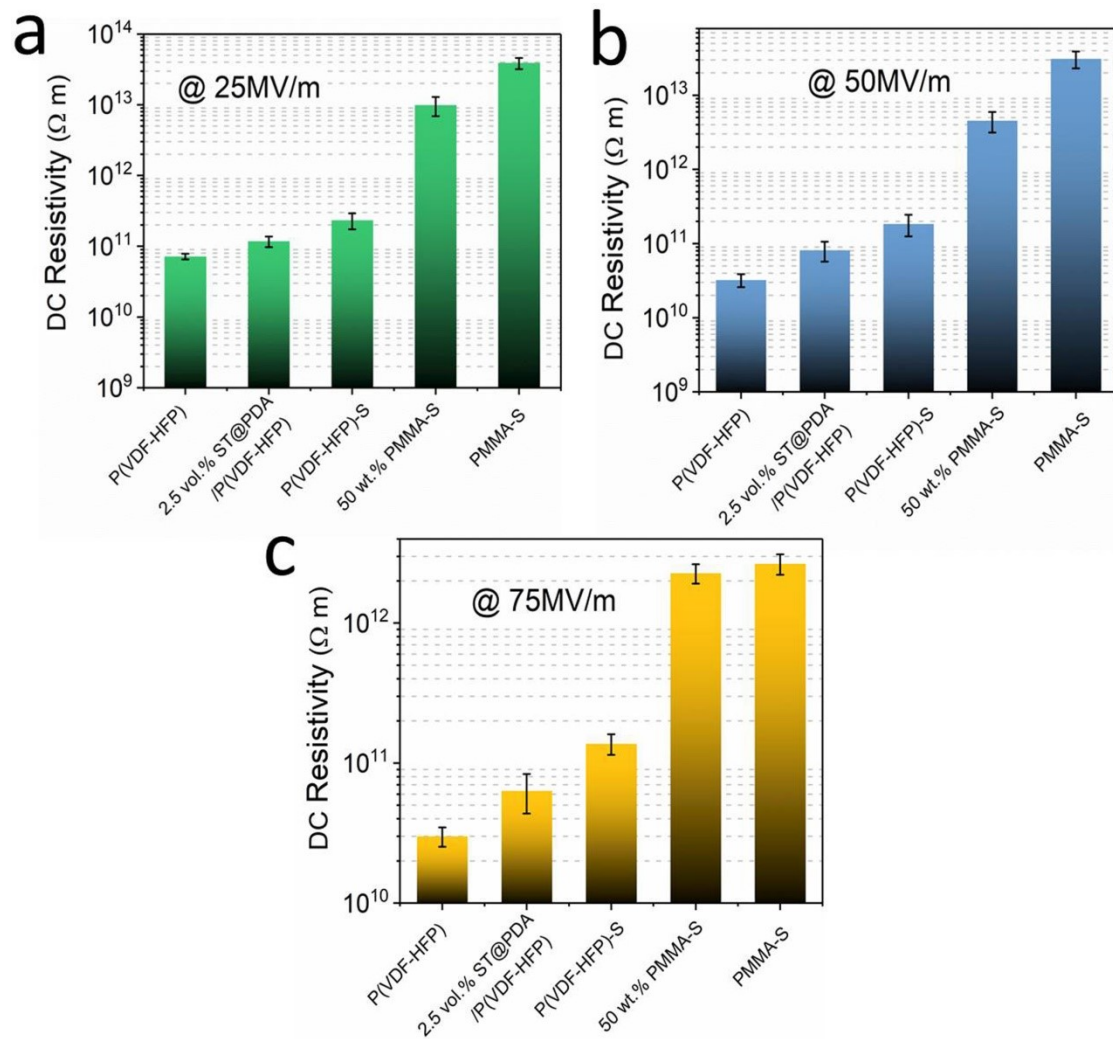


**Fig. S10.** DC electrical resistivity a) measured at 25 MV m<sup>-1</sup>, b) measured at 50 MV m<sup>-1</sup>, and c) measured at 75 MV m<sup>-1</sup> of tri-layered configuration composites, single-layered configuration composite, and pristine P(VDF-HFP).

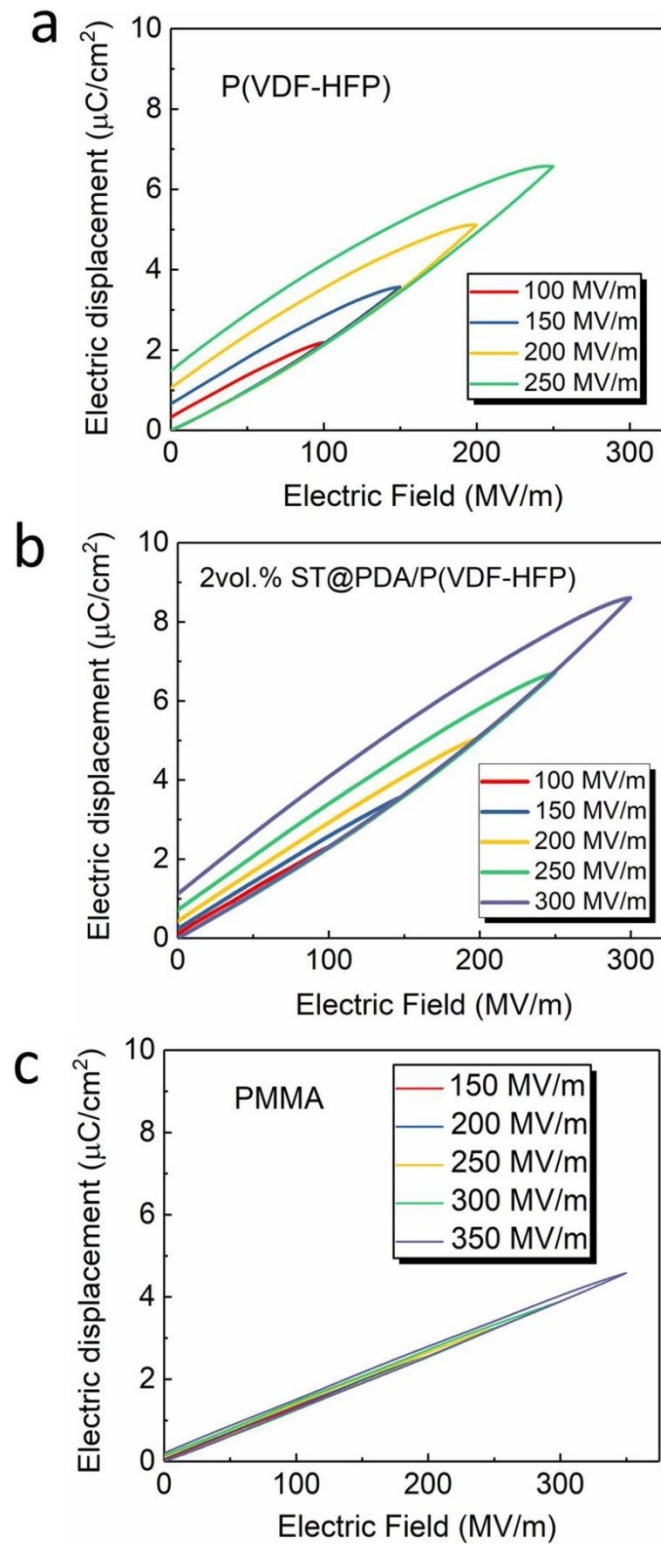


**Fig. S11.** Unipolar electric displacement–electric fields ( $D$ – $E$ ) loops at varied electric fields of a) pristine P(VDF-HFP), b) single layer composite with 2.5 vol.% ST@PDA platelets and c) PMMA.

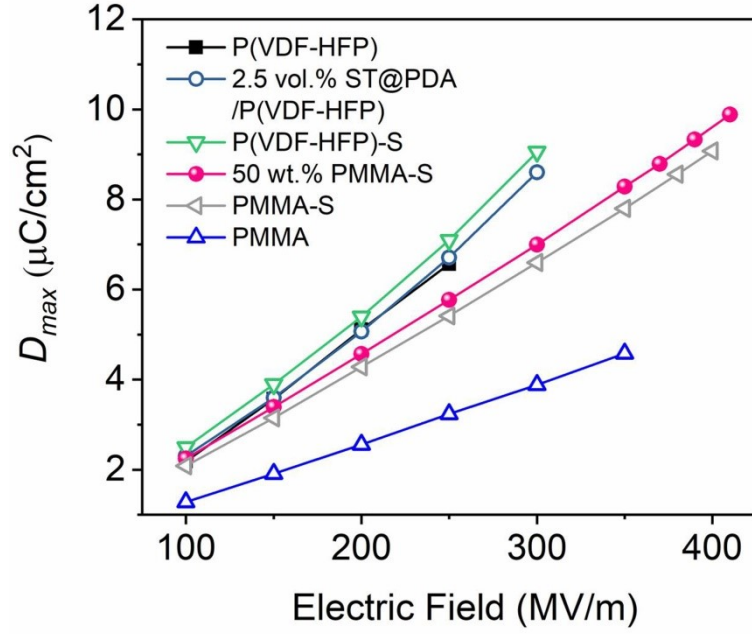


**Fig. S12.** Maximum displacement at varied electric fields of pristine P(VDF-HFP), single layer composite with 2.5 vol.% ST@PDA platelets, and tri-layered composites.

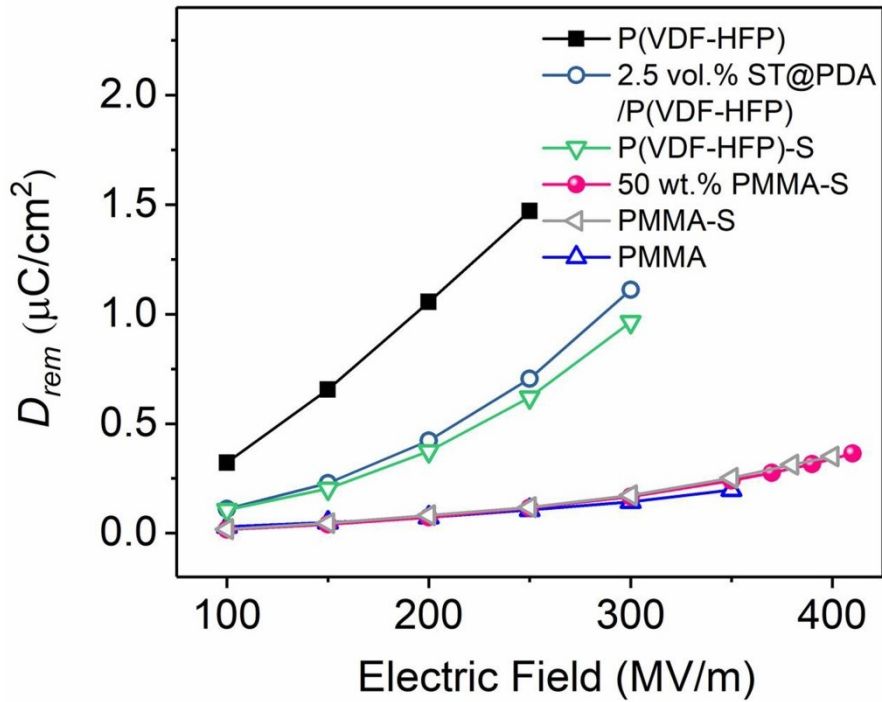


**Fig. S13.** Remnant displacement at varied electric fields of pristine P(VDF-HFP), single layer composite with 2.5 vol.% ST@PDA platelets, and tri-layered composites.

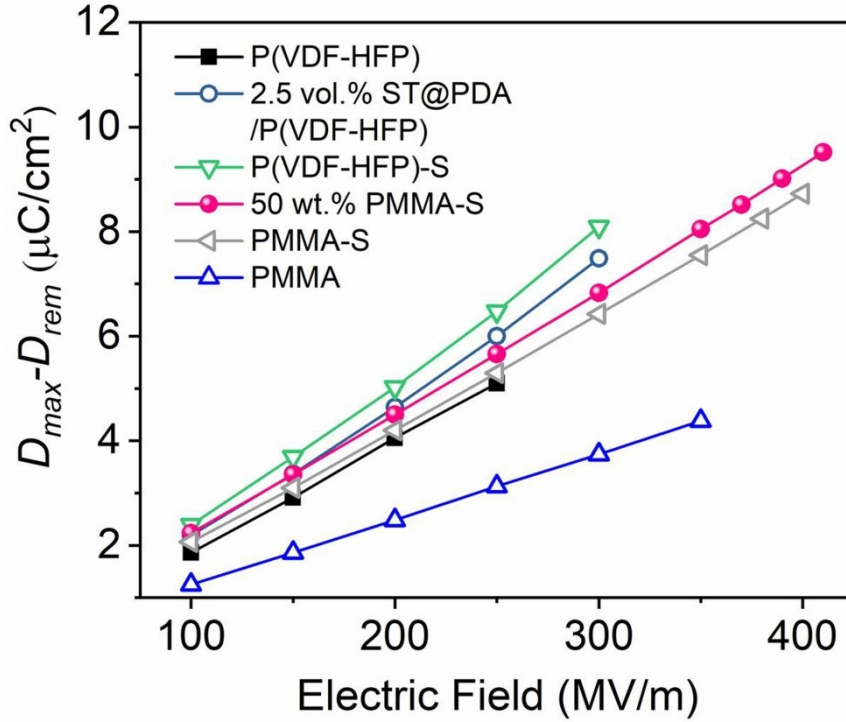


**Fig. S14.** Electric displacement difference at varied electric fields of pristine P(VDF-HFP), single layer composite with 2.5 vol.% ST@PDA platelets, and tri-layered composites.

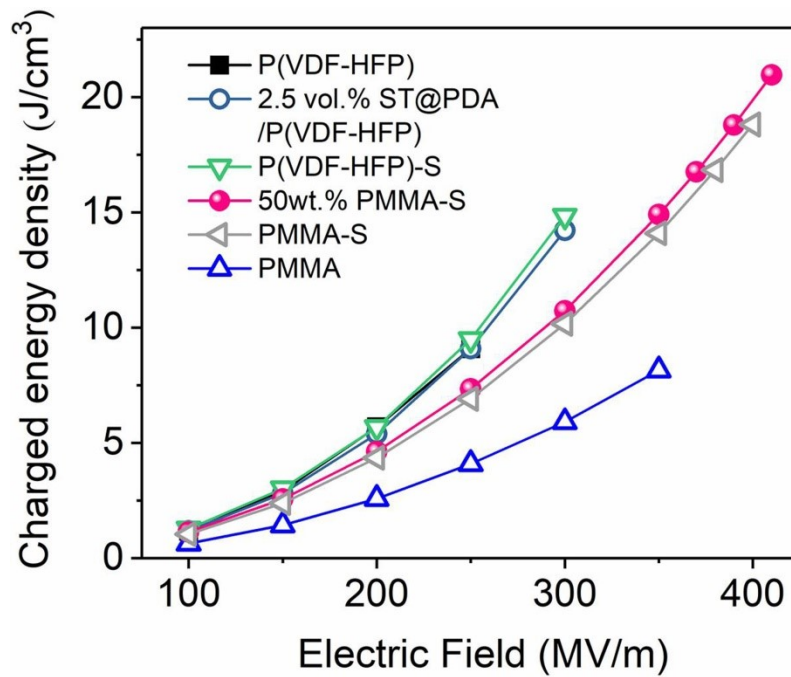


**Fig. S15.** Charged energy density at varied electric fields of pristine P(VDF-HFP), single layer composite with 2.5vol% ST@PDA platelets, and tri-layered composites.

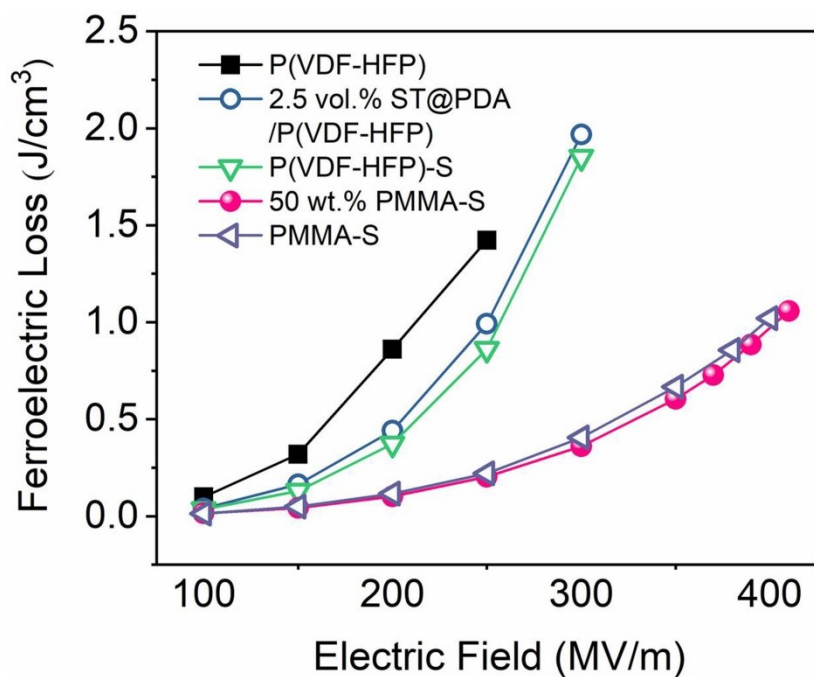


**Fig. S16.** Ferroelectric loss at varied electric fields of pristine P(VDF-HFP), single layer composite with 2.5 vol% ST@PDA platelets, and tri-layered composites.

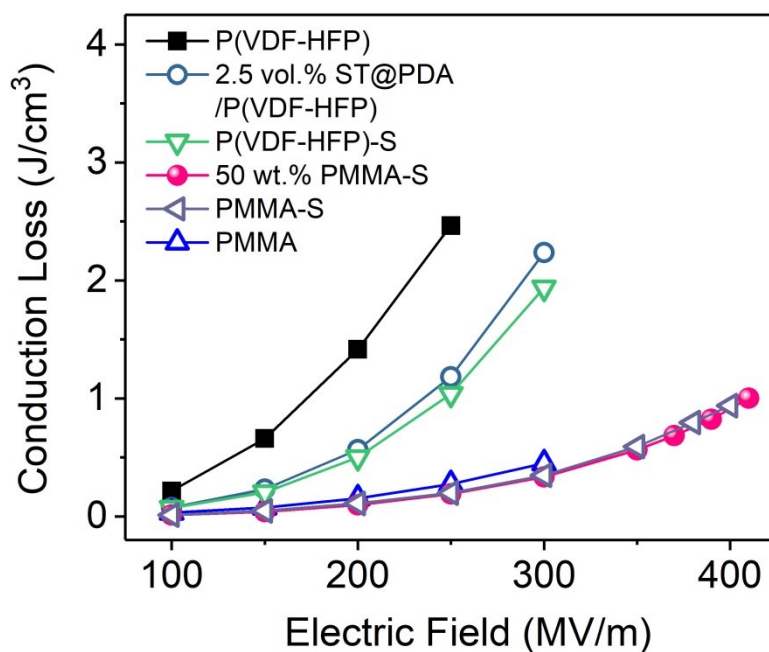


**Fig. S17.** Conduction loss at varied electric fields of pristine P(VDF-HFP), single layer composite with 2.5 vol% ST@PDA platelets, and tri-layered composites.

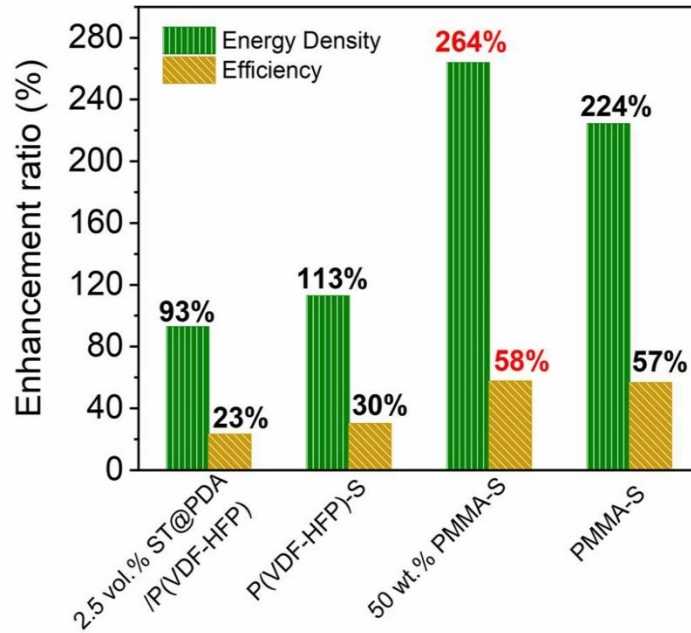


**Fig. S18.** Enhancement ratio at breakdown electric fields of single layer composite with 2.5 vol% ST@PDA platelets and tri-layered composites in comparison with pristine P(VDF-HFP).



**Fig. S19.** Optical image of 50 wt% PMMA-S after winding test (1 month).

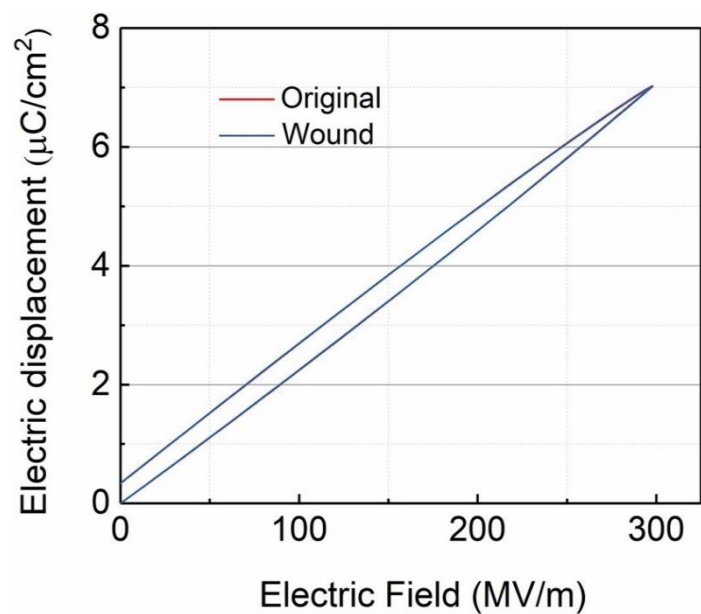


**Fig. S20.** Unipolar electric displacement–electric fields ( $D$ – $E$ ) loops at  $300 \text{ MV m}^{-1}$  of 50 wt% PMMA-S before and after wound tests.

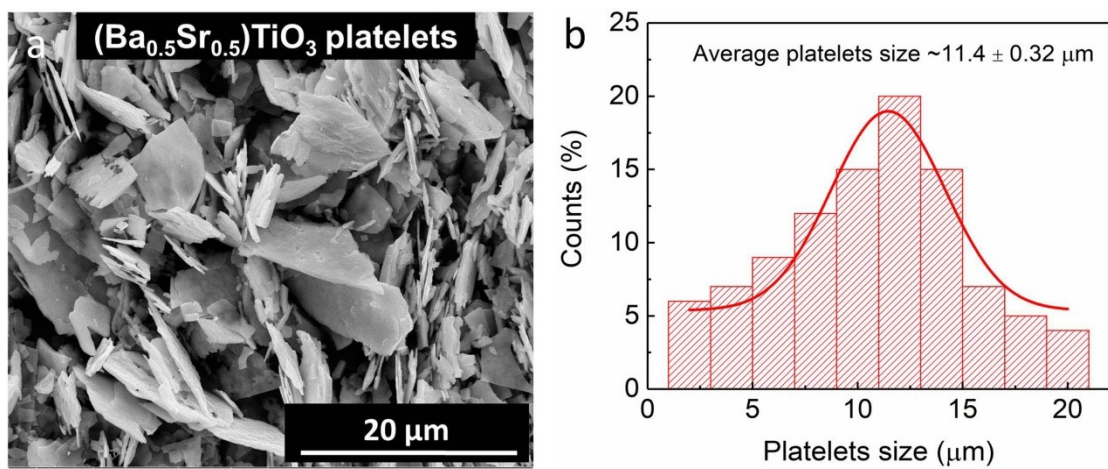


**Fig. S21.** Platelets size distributions of  $\text{Ba}_{0.5}\text{Sr}_{0.5}\text{TiO}_3$  platelets.

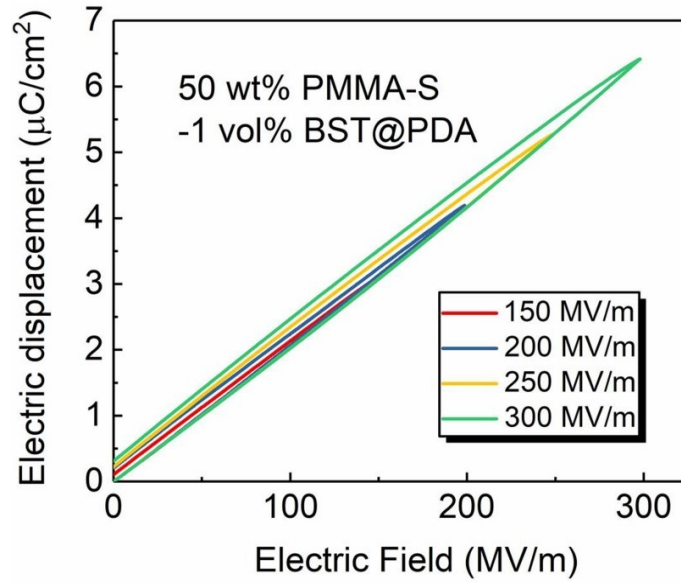


**Fig. S22.** Unipolar electric displacement–electric fields ( $D$ – $E$ ) loops at varied electric fields of 50 wt.% PMMA-S tri-layered composite with 1 vol% BST@PDA plates.

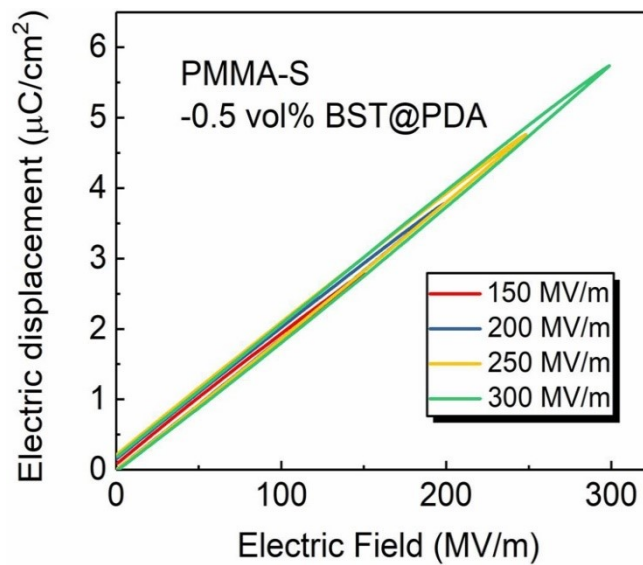


**Fig. S23.** Unipolar electric displacement–electric fields ( $D$ – $E$ ) loops at varied electric fields of PMMA-S tri-layered composite with 0.5 vol% BST@PDA plates.